Int. J. Heat Mass Transfer. Vol. 11, pp. 39–53. Pergamon Press 1968. Printed in Great Britain

COUPLED RADIATION, CONDUCTION AND CONVECTION IN ENTRANCE REGION FLOW

SIMON DESOTO

Rocketdyne, A Division of North American Aviation, Inc., Canoga Park, California

(*Received* 16 *January* 1967)

Abstract—An analytical procedure is developed to investigate the interaction or coupling of radiation with the conduction and convection mechanism in a nonisothermal, nongray gas flowing in the entrance region of a tube with isothermal, black walls. The flow is considered to be hydrodynamically developed and laminar. The radiation was found to drastically affect the temperature distribution and the convective heat transfer in the cylindrical flow field treated. Neither the gray gas assumption nor the transparent gas assumption nor the diffusion approximation is invoked since each was found inadequate. Thus the interlayer absorption effects of a nongray, nonisothermal gas are accounted for in the analysis. Both axial and radial radiative components are included. An exponential band model was used to represent the temperature and frequency dependence of the spectral absorption coefficients. The analysis is not restricted to the use of an exponential band model which was used, as a good example, to represent the radiative properties of CO_2. The exact formulation of the interaction of radiation, conduction, and convection in a flowing, nongray, emitting and absorbing medium is represented by a nonlinear integro-differential equation which was solved numerically. The results of various simplified prediction methods were compared with the exact results obtained.

NOMENCLATURE

A, area [ft^2];
c_p, specific heat at constant pressure [Btu/lbm-°F];
E, emissive power [Btu/ft^2-s];
h, convective heat-transfer coefficient [Btu/ft^2-s-°F];
I, intensity of radiation [Btu/ft^2-s-sr];
k, thermal conductivity [Btu/ft-s-°F];
L, mean beam length [ft];
$\dot{m}$, mass flow rate [lbm/s];
P, pressure [atm];
q, heat-transfer rate [Btu/s];
q/A, heat flux [Btu/ft^2-s];
r, radius [ft];
R_w, tube radius [ft];
R, radius of radiation collection point [ft];
s, coordinate of spherical coordinate system [ft];
T, temperature [°R];
u, axial component of velocity [ft/s];
V, volume [ft^3];
x_c, axial coordinate of cylindrical system [ft];
x_0, axial position of radiation collection point [ft];
x, axial coordinate [ft];
x', y', z', cartesian coordinates [ft].

Greek symbols

α, total absorptivity;
ϵ, total emissivity;
θ, polar angle of spherical coordinate system;
κ_ν, spectral absorption coefficient [ft^2/lbm];
ν, wave number [cm^{-1}];
ν_0, wave number at band head [cm^{-1}];
ρ, mass density [lbm/ft^3];
σ, Stefan–Boltzmann constant [Btu/ft^2-s-°R^4];
τ, optical thickness;
ϕ, φ, azimuthal angle of spherical coordinate system.

Subscripts

B, bulk;

b,	black body;
cond,	conduction;
g,	gas;
r,	radiative;
rad,	radiation;
w,	wall;
ν,	spectral.

Superscripts

ax,	axial component;
rad,	radial component.

INTRODUCTION

THE TREND toward increasing temperatures in modern technological systems has prompted a concerted effort to develop more comprehensive and accurate analytical methods to treat radiation. At present, the importance of such methods is abundantly evident in the development and study of space systems, certain classes of nuclear reactors, rocket combustion chambers and plumes, hypersonic flight and missile reentry, high temperature plasma technology and electric arcs, meteorological problems, burning forests, industrial furnaces and steam generating units. In particular, the interaction or coupling of radiation with conduction and/or convection in radiation emitting and absorbing media has been found to be significant in some of these applications.

Since radiation is, as Hottel has termed it, an "action-at-a-distance" phenomenon which in gases involves interlayer attenuation effects which are dependent on the distributions of temperature, density, frequency, and chemical composition, complications arise because of its three-dimensional character. The analytical difficulties imposed by the interlayer absorption effects can be circumvented by simply ignoring these effects with the use of the transparent gas assumption. For systems of low optical thickness this assumption is realistic. For systems of large optical density the diffusion approximation is generally invoked. The overwhelming interlayer absorption effects in optically dense media reduce the "action-at-a-distance" character of the radiation substantially to a diffusion process, and such an approximation can be successfully applied. In most realistic radiating gas systems, however, the nongray nature of the gas is such that the gas is essentially transparent in the radiating band wings or extremities, while at the same time it is optically dense at the band heads. Thus the complicated frequency dependence of the radiation can change the character of the radiative transport process in a nongray gas from one frequency range to the next. There is no valid approximation for the intermediate optical densities, and the radiative transport in the range of these associated frequencies is the most difficult to treat analytically.

The Goulards [1] studied the interaction of radiation and conduction in the Couette flow of a transparent, gray gas between two isothermal walls at different temperatures. They found that, under these assumptions, the radiation coupling tended to make the temperature gradients in the gas more uniform. Viskanta and Grosh [2] obtained an approximate solution to the same gray gas Couette flow problem by introducing the Rosseland diffusion approximation to convert the integrodifferential energy equation to a differential equation. Thus the Couette flow problem has been solved for a gray gas using the two limiting simplifying assumptions. Adrianov and Shorin [3] treated the case of coupled radiation and convection for a gray gas in laminar flow through a gray isothermal tube. The gas absorptivity was assumed independent of temperature and although the attenuation of radiation from the hot gas to the cold wall was considered, the interchange of radiation between the gas elements was neglected. Gas conduction and the effect of axial temperature gradients were also ignored. Flow between parallel plates was also considered. Einstein [4] used Hottel and Cohen's [5] zoning technique for analyzing heat transfer and temperature distributions in a gray gas flowing within a tube and also between infinite parallel plates. The gas absorptivity was assumed independent of temperature and the

effects of coupled radiation, conduction, and convection were treated with distributed energy sources in the gas. Nichols [6] considered the thermal entrance length problem for turbulent flow of a nongray gas (steam) in an annulus. The interaction of radiation with conduction and convection was studied by assuming interlayer absorption effects based on a mean path length temperature, and gas to gas radiation was ignored in certain regions. The analysis is restricted to cases for which the radiation absorption is small compared to the convection since the solution was obtained by perturbing the solution to an equivalent problem for a nonabsorbing gas. Bevans and Dunkle [7] used a radiation network technique to analyze the radiative energy interchange in a nongray enclosure containing an isothermal, nongray absorbing and emitting gas. Three methods were treated: an exact solution accounting for spectral line structure, a "band energy" approximation in which the smoothed gas bands are separated into a number of frequency intervals such that the radiosity or emissive power varies slowly within each interval, and a gray radiation approximation. They claim that the application of the exact method to "a physical situation is a practical impossibility" due to the very large number of expressions required for a solution. A discrepancy of 63 per cent between the gray and band energy approximations was found for the particular conditions treated, thus emphasizing the weakness of the gray gas assumption. Edwards [8] developed criteria for the selection of band limits to improve the accuracy of band energy methods. An exponential band model developed by Edwards was used by deSoto [9] to analyze the radiative emission from an axisymmetric, nongray, nonisothermal gas system of any optical thickness. The analytic procedure was applied to a nonisobaric rocket exhaust plume which included a surface region of varying chemical composition. An uncoupled analysis of radiation and convection was treated by deSoto and Edwards [10] for the laminar flow of a nongray, nonisothermal gas (CO_2) of any optical thickness in the entrance region of a tube with black walls. The temperature dependence of the spectral absorption coefficients was included. Some of the results obtained in [10] will be compared here with those obtained for the coupled problem. Howell and Perlmutter [11] applied the Monte Carlo method to a nongray, stagnant, nonconducting gas between infinite, parallel, black walls with a one-dimensional temperature distribution.

The analysis and results to be presented involve a nongray gas (CO_2) with all three optical density ranges and with an axisymmetric temperature and density distribution. The radiation interacts with the conduction and convection transport processes for flow in the entrance region of a tube with black, isothermal walls. The inlet gas temperature is uniform with respect to the radius, the tube wall is isothermal, and the velocity–density product is parabolic. The distribution of the axial and radial components of the local radiant heat flux within the gas are computed along with the temperature distribution. Since the method is applied to the entrance region of the tube, the solution might be considered an extension of the classical "Graetz problem" which does not include radiative effects and treats convection and conduction effects in the "entrance region" of a tube with fully developed laminar flow. This problem has been given extensive treatment in the literature [12–14]. It will be shown that at sufficiently elevated temperatures (e.g. 2500°R) the radiation mechanism profoundly alters the temperature distribution and considerably reduces the heat conduction at the wall, while contributing an additional radiant flux.

ANALYSIS

It will be assumed that the flow is hydrodynamically developed, laminar, and steady. This obviates the use of the momentum equation. The axial component of heat conduction is considered negligible and the thermal conductivity is assumed constant. For the conditions treated viscous dissipation and compressi-

bility effects are negligible. There are no heat sources involved except for the nonuniformly distributed emission of radiation from the gas, and chemical reactions or mass diffusion will not be considered. These conditions determine the form of the energy equation. Under these conditions, the local mass velocity ρu becomes $(2\dot{m}/\pi R_w^2)(1 - r^2/R_w^2)$, where $\dot{m}$ is the mass flow rate and R_w is the tube radius. Thus the energy equation reduces to

$$\frac{2\dot{m}}{\pi R_w^2}\left(1 - \frac{r^2}{R_w^2}\right) c_p \frac{\partial T}{\partial x} + \frac{\partial[(q/A)_r^{ax}]}{\partial x} + \frac{1}{r}\frac{\partial[r(q/A)_r^{rad}]}{\partial r} = \frac{k}{r}\frac{\partial[r(\partial T/\partial r)]}{\partial r}. \quad (1)$$

Equation (1) is an integrodifferential equation since the radiation terms must be expressed in terms of functions involving multiple integrals. The development of these radiation integrals will now be discussed briefly in the section that follows.

Radiative transfer

In developing the radiation integrals it will be assumed that scattering effects are negligible and that the index of refraction is unity; i.e. an infinitesimal mass element of gas does not alter the direction of the incoming radiation. These are realistic assumptions for radiation in gases in the infrared range. Further, local thermodynamic equilibrium is assumed to exist. Therefore the equation of transfer may be written [15]

$$-\frac{1}{\rho(s)\kappa_\nu(s)}\frac{dI_\nu(s)}{ds} = I_\nu(s) - I_{b\nu}(s). \quad (2)$$

Equation (2) is a nonhomogeneous equation whose solution may be found by the method of variation of parameters. For an internal point in a gas bounded by walls the solution may be shown to consist of two pairs of spectral intensity terms, one pair in the positive sense and one in the negative sense, which may be written as follows:

$$I_{\nu_{gas}}^- = \int_0^{s_{w1}} \rho\kappa_\nu I_{b\nu} \exp\left[-\int_0^s \rho\kappa_\nu \, ds'\right] ds \quad (3)$$

$$I_{\nu_{wall}}^- = I_{w1\nu} \exp\left[-\int_0^{s_{w1}} \rho\kappa_\nu \, ds\right]. \quad (4)$$

The subscript $w1$ refers to that part of the tube wall below the $x' - z'$ plane, whereas $w2$ [in equations (5) and (6)] refers to the tube surface above the $x' - z'$ plane in Fig. 1. The term $I_{\nu_{gas}}^-$ represents the spectral intensity at the area element dA (see Fig. 1) due to the emission and

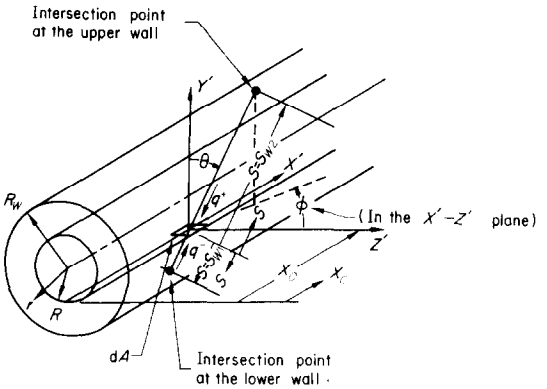

The subscript W1 refers to that part of the tube wall below the X'-Z' plane
The subscript W2 refers to the tube surface above the X'-Z' plane

FIG. 1. The tube geometry.

interlayer absorption effects of the gas along a line of sight in the region *below* the $x' - z'$ plane. The term $I_{\nu_{wall}}^-$ represents the spectral intensity at the area element dA due to wall emission at the end of the line of sight in the region *below* the $x' - z'$ plane after accounting for the absorption effects of the intervening gas elements. The corresponding expressions for the intensities in the q^+ direction are

$$I_{\nu_{gas}}^+ = \int_0^{s_{w2}} \rho\kappa_\nu I_{b\nu} \exp\left[-\int_0^s \rho\kappa_\nu \, ds'\right] ds \quad (5)$$

$$I_{\nu_{wall}}^+ = I_{w2\nu} \exp\left[-\int_0^{s_{w2}} \rho\kappa_\nu \, ds\right]. \quad (6)$$

The spectral radiant heat flux may be expressed as

$$q_\nu/A = q_\nu^+/A - q_\nu^-/A = \iint_{\phi\theta} (I_\nu^+ - I_\nu^-) \sin\theta \cos\theta \, d\theta \, d\phi \quad (7)$$

where

$$I_\nu^+ = I_{\nu_{gas}}^+ + I_{\nu_{wall}}^+ \tag{8}$$

$$I_\nu^- = I_{\nu_{gas}}^- + I_{\nu_{wall}}^-. \tag{9}$$

When equations (3–6) are substituted in equation (7) and an integration over all wave numbers is performed, there results

$$\begin{aligned} q/A &= q^+/A - q^-/A \\ &= 2\int_0^\infty \int_{-\pi/2}^{\pi/2} \int_0^{\pi/2} \Big[I_{w2\nu} \exp\Big(-\int_0^{s_{w2}} \rho\kappa_\nu \, ds\Big) \\ &+ \int_0^{s_{w2}} \rho\kappa_\nu I_{b\nu} \exp\Big(-\int_0^{s} \rho\kappa_\nu \, ds'\Big) ds\Big] \\ &\times \sin\theta \cos\theta \, d\theta \, d\phi \, d\nu \\ &- 2\int_0^\infty \int_{\pi/2}^{3\pi/2} \int_{\pi}^{\pi/2} \Big[I_{w1\nu} \exp\Big(-\int_0^{s_{w1}} \rho\kappa_\nu ds\Big) \\ &+ \int_0^{s_{w1}} \rho\kappa_\nu I_{b\nu} \exp\Big(-\int_0^{s} \rho\kappa_\nu \, ds'\Big) ds\Big] \\ &\times \sin\theta \cos\theta \, d\theta \, d\phi \, d\nu. \end{aligned} \tag{10}$$

Equation (10) represents the local radiative heat flux passing by any interior infinitesimal area element within the gas system. Actually the limits of the angular coordinates in equation (10) imply that this area element is oriented as shown in Figs. 1 and 2. Hence equation (10) and the development shown above apply strictly to the radial component of the radiative heat flux. However both the $(q/A)_r^{ax}$ term and the $(q/A)_r^{rad}$ term in equation (1) can be expressed as equation (10) except that the variables θ and ϕ and their limits are defined differently for each case. Figure 3 defines these variables and their limits for the axial component, and Fig. 2 describes them for the radial component. The variables θ and ϕ are two of the coordinates of a spherical coordinate system.

The spherical coordinate system (s, θ, ϕ) used in Figs. 1–3 seems to be the natural system to express radiation phenomena. The area element receiving the local value of the radiative flux may conveniently be located at the center of such a system. Due to interlayer absorption effects, those volume elements nearer the radiation collection point exert a more prominent effect on the radiation at the collection point. These volume elements should therefore be smaller. The spherical system automatically satisfies this condition. For a transparent medium, a fixed pencil of radiation or solid angle with its apex at the collection point requires no correction for an "inverse square attenuation" effect.

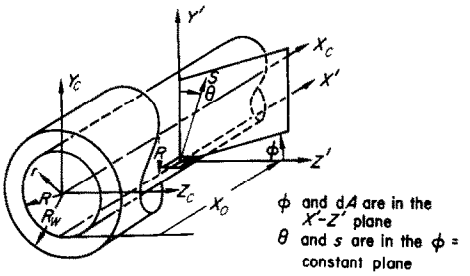

FIG. 2. The geometry for the radial radiative component.

Since the property distributions in the tube flow are most conveniently expressed in terms of cylindrical coordinates, a coordinate transformation from the spherical system to the cylindrical system is necessary. For the radial radiative component, this transformation is

$$r = [s^2(\cos^2\theta + \cos^2\phi \sin^2\theta) - 2RS\cos\theta + R^2]^{\frac{1}{2}} \tag{11}$$

and

$$x_c = s \sin\theta \sin\phi + x_0. \tag{12}$$

For the axial radiative component the corresponding transformation equations are

$$r = [s^2 \sin^2\theta - 2sR \sin\theta \cos\phi + R^2]^{\frac{1}{2}} \tag{13}$$

and

$$x_c = s\cos\theta + x_0. \tag{14}$$

The above coordinates are described in Figs. 2 and 3. As far as the calculation procedure is concerned, this means that a different geometric transformation would be required for the radial and axial radiative components. That is, equations (11) and (12) would be used in conjunction

with equation (10) for the radial component of the radiative flux, whereas equations (13) and (14) would be used for the axial component.

If a separate coordinate transformation is used to evaluate both the radial and axial components of the radiative flux, the computer execution time is essentially doubled since a separate line of sight integration process is necessary for each of these components. Under

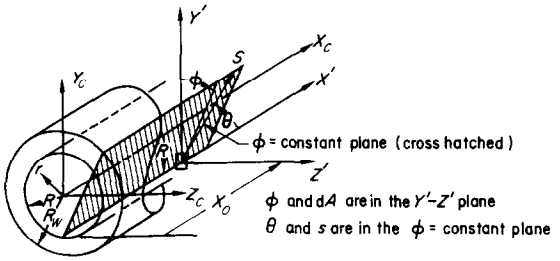

FIG. 3. The geometry for the axial radiative component.

such circumstances a different set of points in the three-dimensional space would be scanned in each case. This time consuming duplication of the lengthy integration process is unnecessary. It is possible to simultaneously calculate both the axial and radial components of the radiative flux by performing only a single set of line of sight integrations, i.e. by scanning the three-dimensional space only once. This procedure can be explained briefly as follows.

Although the limits of equation (10) apply only for the radial radiative components, the form of the integrand is the same for both axial and radial components. It is noted that the term $\sin\theta\,\mathrm{d}\theta\,\mathrm{d}\phi$ in the integrals of equation (10) represents an infinitesimal solid angle increment. The superscript r is appended to this term for the radial component system in Fig. 2 and the superscript a for the axial component system in Fig. 3. The same set of solid angle increments and their associated lines of sight may be used for evaluating both the axial and radial radiative components. Hence

$$(\sin\theta\,\mathrm{d}\theta\,\mathrm{d}\phi)^r = (\sin\theta\,\mathrm{d}\theta\,\mathrm{d}\phi)^a. \quad (15)$$

Now $(\cos\theta)^a$ may be expressed in terms of $(\theta)^r$ and $(\phi)^r$ by equating equations (12) and (14). Since a given point on a particular line of sight will have common values of x_c, s and x_0 whether the axial contribution or radial contribution is being computed, there results

$$(\cos\theta)^a = (\sin\theta\sin\phi)^r \quad (0 \leqslant \theta_a \leqslant \pi) \quad (16)$$

Hence

$$(\sin\theta\cos\theta\,\mathrm{d}\theta\,\mathrm{d}\phi)^a = (\sin^2\theta\sin\phi\,\mathrm{d}\theta\,\mathrm{d}\phi)^r. \quad (17)$$

If the superscript a were appended to the θ and ϕ variables in equation (10), this equation would then represent the axial component of the radiative heat transfer in the system shown in Fig. 3 (the θ and ϕ limits would be changed to correspond). Equation (17) is then substituted in equation (10) to obtain an expression for $(q/A)_r^{ax}$ in the spherical system (s, θ, ϕ) shown in Fig. 2 and the axial component may be evaluated along with the radial component in the same spherical system associated with the radial component.

Due to the complexity of the integrodifferential energy equation [equation (1)], in which the coupling of the temperature and radiative flux distributions is apparent, a numerical solution is necessary. The numerical solution technique chosen is iterative in nature. First a temperature distribution is estimated (e.g. the Graetz distribution) and the radiative flux distribution is computed by evaluating equation (10) by a trapezoidal multiple integration. When the net radiative flux distribution is known, the temperature distribution is computed by solving equation (1) with a finite difference method. A new radiative flux distribution is then computed along with a new temperature distribution. This procedure is iterated until an acceptable degree of convergence is attained. Four iterations were required to obtain the results to be shown.

An exponential band model for CO_2, developed by Edwards and Menard [16], was used to produce values of the spectral absorption coefficient as a function of temperature and wave number. This model, which was used to

correlate data for temperatures below approximately 2500°R, is described by the equation

$$\kappa_\nu = \frac{C_1}{C_3}\left(\frac{180}{T}\right)^n \exp\left[\frac{-|\nu_0 - \nu|}{C_3}\left(\frac{180}{T}\right)^{\bar{n}}\right] \tag{18}$$

where $n = \frac{1}{2}$ and $C_1 = 4{\cdot}7$, 110 and 19 (cm^{-1}/g-m^{-2}) for the 2·7, 4·3 and 15 μ bands respectively; $C_3 = 22$, 11·5 and 12·9 (cm^{-1}) for the 2·7, 4·3 and 15 μ bands respectively; $\nu_0 =$ 3750, 2435 and 667 (cm^{-1}) for the 2·7, 4·3 and 15 μ bands respectively. The band model is described more fully in [16].

RESULTS

The results obtained are shown graphically in Figs. 4–10. Constant values of the thermal conductivity and specific heat were taken for the conduction and convection terms in the energy equation. Values of $c_p = 0{\cdot}285$ Btu/lbm-°F and $k = 0{\cdot}03$ Btu/h-°F-ft were selected (corresponding to the properties of CO_2 at a mean temperature of 1500°R). The mass flow rate used was 10 lbm/h in the 2-in dia. tube treated. This produced a maximum centerline velocity (at the tube exit) less than 10·6 ft/s at the pressure of one atmosphere assumed to exist in the tube. Thus compressibility effects were safely neglected. The optical length based on the tube diameter varied from a value of essentially zero in the band wings to a maximum value of fifty-two at the head of the 4·3 μ band and at the temperature existing at the tube entrance (530°R). The local densities were computed, with the perfect gas equation of state, everywhere in the gas to determine the optical

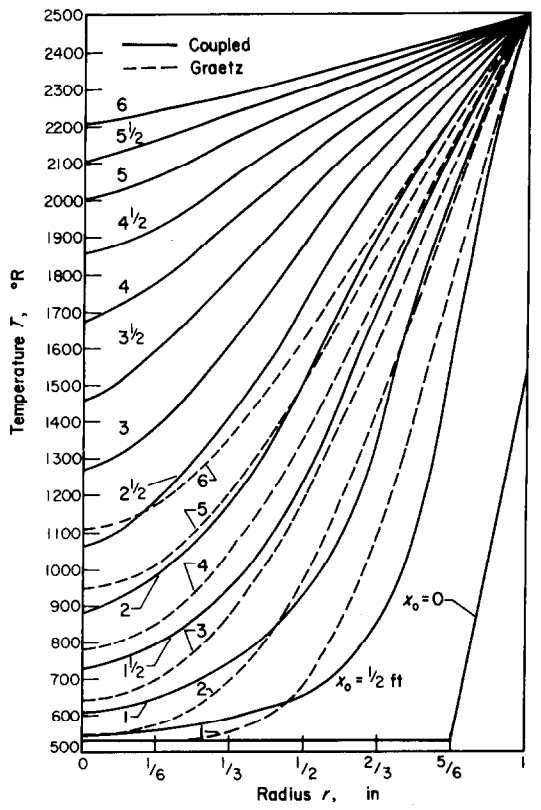

FIG. 4. $T(r, x)$ for the coupled tube problem and the Graetz problem.

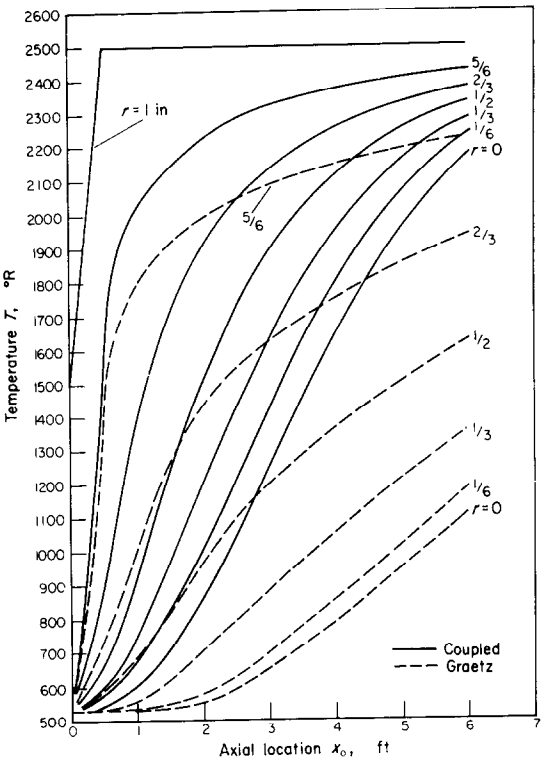

FIG. 5. $T(x, r)$ for the coupled tube problem and the Graetz problem.

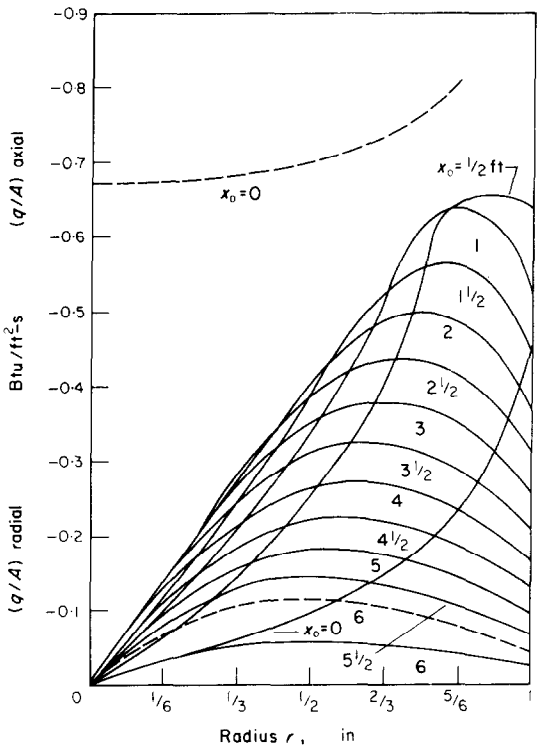

FIG. 6. Radiative heat flux distribution.

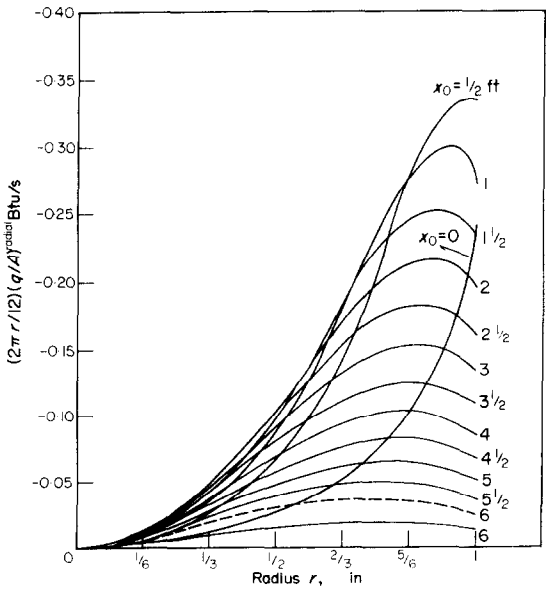

FIG. 7. Local radiative heat-transfer rate.

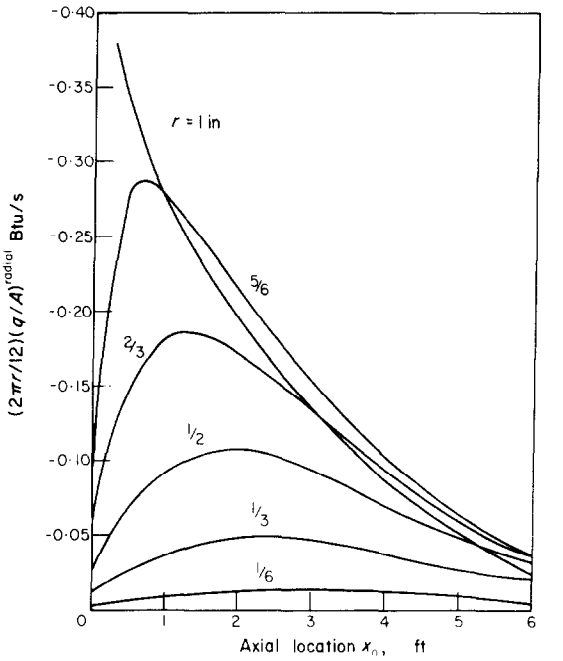

FIG. 8. Local radiative heat-transfer rate.

thickness increments in the radiation integrals. The tube wall temperature was taken as 2500°R and the inlet gas temperature and pressure were 530°R and one atmosphere. The above input parameters produced a Reynolds number of 1000, hence the velocity profile, as has been mentioned elsewhere, was taken as laminar and fully developed. The tube dimensions used were 2 in. in diameter and 6 ft in length. This 36 to 1 length to diameter ratio was sufficient to include all of the interesting entrance effects. The radius was divided into six equal increments and tube length into twelve equal increments (a "six by twelve mesh"). A black porous disk was assumed to exist at both ends of the tube. The temperature of the inlet disk was taken as the inlet gas temperature while the temperature of the disk at the discharge end was taken as the wall temperature. These conditions were chosen to produce convenient but reasonable boundary conditions for the radiation terms at the ends of the tube. Although the discharge disk in particular might be considered somewhat artificial, it fairly well simulates an elbow located

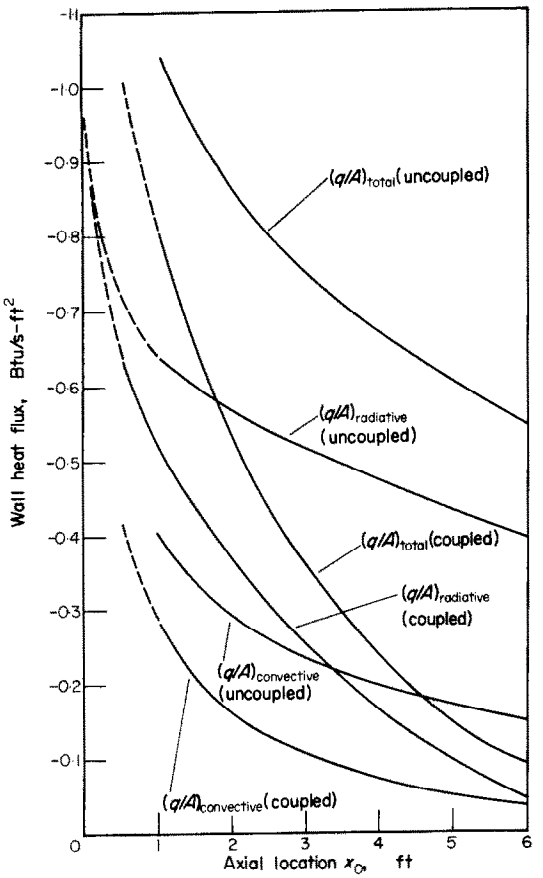

FIG. 9. Local heat flux at the wall.

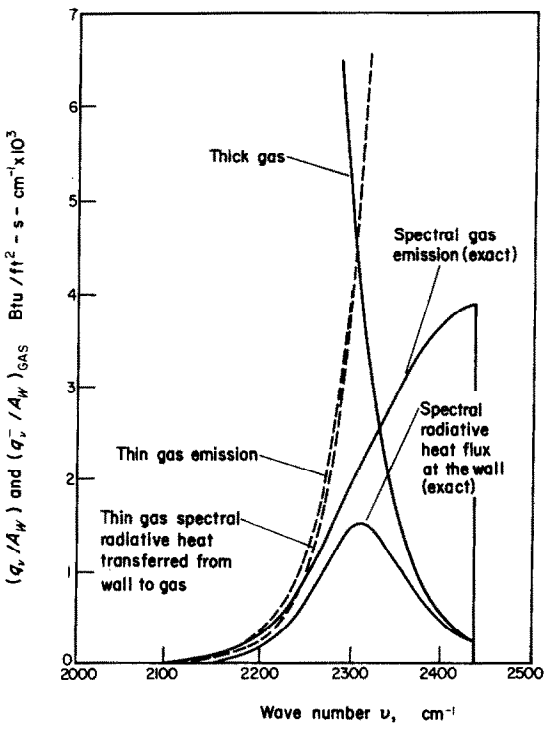

FIG. 10. Comparison of the thick and thin gas approximations with the exact results, hot wall–cold gas.

at the end of the tube. Due to geometrical considerations alone, the local radiation to any point in the gas is not significantly affected by conditions existing more than three to six diameters away. Hence the temperature distributions, computed at the positions 5 and $5\frac{1}{2}$ ft downstream of the tube entrance, are essentially unaffected by the disk assumption.

The question of using dimensionless parameters suggests itself. It seems appropriate to immediately state that a dimensionless treatment would require first of all a geometric similitude. Further, the boundary conditions must be similar. As pointed out by Goulard the reduced properties must be a function of the other properties only in their reduced form. Goulard concludes as follows: "Similitude is not a precise tool in the general case of radiation gas dynamics. However, many cases of interest fall within asymptotic cases where some terms vanish, or simpler expressions can be used, or simplified representations can be allowed for a limited range of properties." Such simplified representations, for example, involve the gray gas assumption, or the thin gas assumption, or the thick gas assumption. It has been found, however, that these assumptions are not realistic for the case to be treated here, which involves intermediate optical thicknesses. The frequency dependence of the nongray gas also complicates matters considerably. This is especially true when the spectral absorption coefficients are also temperature dependent. Thus, all other conditions being similar, two different gases whose absorption coefficients have a different frequency and temperature dependence would

produce different effects as a result of this dependence. Since for most common gases, such as CO_2 this functional relationship can be expressed only with approximate models, a dimensionless treatment would only apply for a particular model of a particular gas. Thus its utility is very limited, and the results of this investigation are left in dimensional form.

DISCUSSION

The computed temperature distribution for the coupled tube problem is shown in Fig. 4 as a function of the radius with x as a parameter. The solid lines represent the results of the coupled analysis, while the superimposed dashed lines represent the Graetz distribution in which radiation effects are ignored. The inclusion of the radiative effects is seen to produce a drastic difference in the results. Figure 5 shows the same distributions plotted as a function of the axial position x with the radius r as a parameter. The radial component of the radiative flux (Btu/s-ft^2) as a function of r and x is plotted in Fig. 6, and the corresponding radiative heat-transfer rate (Btu/s) is shown in Figs. 7 and 8. The distribution for $x = 6$ ft is shown twice in Figs. 6 and 7. The solid lines were obtained directly from the calculated results and reflect the artificial effect of the black porous disk at the wall temperature assumed to exist at the downstream end of the tube. The dotted lines were obtained by simply extrapolating the curves of Fig. 8 past $5\frac{1}{2}$ ft, and are approximately the distributions that would have been predicted had the tube length been extended so as not to impose the porous disk effect at $x = 6$ ft.

The distribution of the axial radiative component at the tube entrance is shown as the dotted line in the upper region of Fig. 6. The computed values of the axial radiative component at the positions $x \geqslant \frac{1}{2}$ ft were found to be so small as not to warrant plotting on Fig. 6. Thus, it was found that although the axial radiative component is large at the tube entrance, it decreases rather abruptly as the flow proceeds only a short distance into the tube and its effect thereafter is very small. Figure 5 shows that the axial component of the heat conduction (the slope of the curves) is large at the tube entrance (at the larger values of the radius) and decreases sharply as the flow proceeds downstream. The influence of the axial components therefore is expected to be small throughout the tube except for that small region near the inlet disk in which the effects of the axial components are felt, for a very short interval, and subsequently diffused in the downstream direction by the convection mechanism. The effect of the axial component of radiation was checked by exercising a program option which deletes the axial component from the energy equation and a negligible change was found in the temperature response shown, which includes the effects of both axial and radial radiative components.

The conductive and radiative heat fluxes at the wall, along with the sum of these two fluxes (the total heat transfer), are shown plotted in Fig. 9 at various axial positions for both the coupled and uncoupled conditions. The uncoupled radiative flux was obtained from the results of an uncoupled tube program [10]. The Graetz temperature distribution computed for the uncoupled problem was used to deduce the local conduction at the wall.

It is interesting to note that Figs. 6 and 7 indicate a maximum radiative heat flux and radiative heat-transfer rate, respectively, existing in the gas interior at progressively smaller radii as the flow proceeds into the tube. This effect can be easily explained with the following simplified concept of the flow field: If for the moment the flow in the tube were assumed to be comprised of only two distinct zones, a cold core of gas and a hot "thermal boundary layer", then the local radiative heat-transfer rate from wall to gas in the hot boundary layer will be decreased by the effect of the reradiation from the hot boundary layer back to the wall. Due to symmetry the net radiative flux or heat-transfer rate at the axis is zero. Hence the maximum will exist neither at the wall nor at the axis of

symmetry. For such a simplified system, the maximum net radiative heat-transfer rate will occur in the cold region in the vicinity of the interface between the cold gas core and the hot boundary layer. Since the thermal boundary-layer thickness increases as the entrance region flow proceeds downstream, both the maximum radiative heat flux and radiative heat-transfer rate exist at progressively smaller values of the radius as shown in Figs. 6 and 7. Although the true flow pattern does not consist of two distinct regions as imagined above, the same qualitative argument is still valid. It is worth mentioning at this point that in evaluating the local absorption of energy, the heat-transfer rate (energy per unit time) is more significant than the heat flux (energy per unit time per unit area). In considering the energy absorption effects for flows between flat plates, for example, the heat flux is directly proportional to the heat-transfer rate, whereas for flow in a tube, a uniformly distributed heat-transfer rate, with respect to the radius, produces a heat flux which is inversely proportional to the radius. Thus the change in the heat-transfer rate (radiative or conductive, etc.) rather than the change in the heat flux is a more meaningful measure of the energy absorbed or rejected locally. This can be seen by interpreting the energy equation.

Near the entrance of the tube, at $x_0 = \frac{1}{2}$ ft, say, the radiation emitted by the wall is quickly absorbed by the cold gas core as this radiation migrates from the wall toward the tube axis. This is shown by the sharp decrease (moving from right to left) in the curves in Figs. 6 and 7 at $x_0 = \frac{1}{2}$ ft. For this axial location the high rate of radiation absorption exists at radii less than $\frac{5}{6}$ in or so. The maximum rate of radiation absorption exists at the inflection points, i.e. points of maximum slope, of the curves shown in Fig. 7. The sharp temperature gradients, at the various axial positions, that produce this effect can be seen in Fig. 4. The negative slopes, of the curves in Fig. 7, to the right of the maxima indicate that in these "radiation boundary layer" regions near the wall there is a net radiative emission from the gas rather than an absorption. Since by the Second Law this radiative heat transfer cannot flow to the hotter wall, it must be emitted toward the cooler gas core. The net radiant heat emitted by this hot boundary layer in the gas is more than compensated for by the effect of conduction from the wall. Thus in spite of the radiant heat emitted by this layer, its temperature increases steadily, at a constant radius, in the direction of flow, as can be seen in Fig. 4. All modes of heat transfer must obey the Second Law. They must individually flow in the direction of the decreasing temperature gradient. Further, it is interesting to note that the orthogonal components of each energy flow mode interact with each other, as well as with the other modes of energy flow. The significant absorption of radiation in regions near the inflection points of Fig. 7 affects the temperature distribution. Thus the S-shaped curves in Fig. 4 are bowed concave downward more pronouncedly than the equivalent Graetz profiles (shown dotted). Even the Graetz profiles are bowed slightly concave downward in this region. The net result is that the local conduction at the wall is decreased because of the interaction of the radiation mechanism. This effect is shown quantitatively in Fig. 9.

It is interesting to study the characteristics of the curves in Fig. 8 in view of the integral form of the energy equation. If the axial component of the radiative heat transfer is neglected, the above energy equation may be integrated with respect to the radius between a lower limit r_1 and an upper limit r_2 to give

$$\frac{\partial}{\partial x}\left[c_p \int_{r_1}^{r_2} \rho u T r \, dr\right] = r_1[(q/A)_{\text{cond}} + (q/A)_{\text{rad}}]_{r_1} - r_2[(q/A)_{\text{cond}} + (q/A)_{\text{rad}}]_{r_2}. \quad (19)$$

Fluxes in the negative r and x directions are taken as negative. The above equation implies that for an annulus of gas, existing in the steady state and of unit axial length with an outer radius r_2 and an inner radius r_1, the increase in

the fluid enthalpy as it flows downstream is due to a net transfer of both heat conduction and radiation. Let the outer radius of the annulus be taken as the tube wall radius and let the inner radius be taken as any other. Figure 8 indicates that the curve for the 1-in radius (the wall radius) intersects three of the curves shown, within the 6-ft tube length. The crossover point for the one-inch curve and the curve at $\frac{5}{6}$ in lies at an axial position slightly less than 1 ft. This means that downstream of this axial location, an annulus of gas bounded by the wall and by an inner cylindrical surface at a radius of $\frac{5}{6}$ in, the radiative heat flux emitted by this annulus to the cooler gas core exceeds the radiative heat flux that this annulus receives from the wall. Since the convection term is increasing, the conduction to the annulus from the wall exceeds the conduction from the annulus to the cooler gas core. As the flow progresses further and further downstream, the inner radius of the annulus of gas, which radiates more heat than it receives from the wall, decreases until it reaches the centerline in the limit as the axial location approaches infinity. Thus, as the curve at a radius of one inch in Fig. 8 asymptotically approaches the x axis at infinity, as do all the other curves, it will have crossed all the other curves.

It has been mentioned that the heat conduction at the wall is decreased due to the interaction of the heat-transfer mechanisms. It was found that the thickening of the thermal boundary layer by the radiative transfer effect produces a lower radiative heat flux from wall to gas for the coupled analysis than would have been computed on the basis of the original Graetz (or uncoupled) temperature profiles. This effect is shown in Fig. 9. Thus (for the hot wall–cold gas case treated) the interaction or coupling of radiation produces a lower value of both the radiative heat flux and the conductive heat flux at the wall than would have been predicted by the use of the uncoupled (Graetz) temperature profiles that are computed on the basis of conduction and convection alone. The sum of the radiative and conductive fluxes at the wall represents the total heat flux there and, as can be seen in Fig. 9, there is a drastic difference between the total fluxes computed on a coupled and an uncoupled basis. This difference is greater at the axial positions further downstream because, as can be seen in Fig. 4, the temperature distribution at $x_0 = 6$ ft, for the coupled analysis, is almost isothermal while for the uncoupled case the temperature gradients are still relatively high.

In Fig. 9 the radiative flux alone computed for the uncoupled case is seen to be much larger than the total flux for the coupled condition for x_0 larger than 2 ft. This reflects the relatively high rate of temperature response in the coupled case due to the relatively strong absorption of radiation by the gas at the lower values of x_0. The gross error that can be made in predicting the local heat flux to the wall, in the entrance region, when the radiation mechanism is completely ignored is seen in Fig. 9 by comparing the uncoupled convective heat flux distribution with the total heat flux distribution for the coupled case.

A comparison with a crude approach

In order to compare the results of the coupled solution with results that might be obtained by a simplified estimate which involves the calculation of the uncoupled convective effect and an uncoupled radiative effect, the following "crude" equation was used:

$$(q/A)_{\text{local}} = h(T_w - T_B) + \sigma(\alpha_g T_w^4 - \epsilon_g T_B^4). \tag{20}$$

The local convective heat-transfer coefficient h was obtained from the classical Graetz problem solution. Following Hottel's recommendation [17], the total absorptivity, α_g, of the gas was evaluated at T_w and at $PL(T_w/T_B)$, rather than at PL, and the result was multiplied by $(T_B/T_w)^{0.65}$. The total emissivity of the gas was evaluated at a temperature "representative" of the distribution in the gas (e.g. the bulk temperature). These values of the total absorptivity and emissivity were obtained from a chart which was deduced

by an integration over all wave numbers involving the spectral absorption coefficients used. In order to assess the effects of an uncoupled solution based on total emissivities and absorptivities, the bulk temperatures used were those obtained from the coupled problem solution. Table 1 shows the values (A) of the local heat flux obtained with this crude uncoupled method along with the values (B) obtained from the coupled problem solution, i.e. Fig. 9. It is seen from Table 1 that the approximate method is inadequate.

It is seen that the thin gas approximation overestimates both the gas emission and the radiative heat flux at all wave numbers except for a small spectral region in the band wing where the spectral absorption coefficients are very low. This overestimation exists simply because interlayer absorption is ignored in the approximation. The diffusion approximation correlates the radiative heat flux rather well for a small spectral region near the band head where the optical densities are high, but produces values which are much too high over the rest of the band. This behavior is due simply to the fact that the thick gas approximation accounts only for local conditions at the wall and ignores the different temperature levels existing at the gas core. It was speculated that the thin and thick gas approximations might be used to construct a simulated band response with the band peak represented by the intersection point of the two curves. This could be done with much less effort than required by the more exact calculations. But for the case shown in Fig. 10 the simplified prediction would be too high by a factor of roughly two. Thus for nongray gases of high, low, and intermediate optical densities, both the transparent gas approximation and the diffusion approximation are seen to produce significant errors in some spectral region.

Table 1

x_0	1	2	3	4	5	6
(A) $(q/A)_{\text{local}}$ equation (20)	1·2	0·96	0·73	0·47	0·31	0·22
(B) $(q/A)_{\text{local}}$ Fig. 9	0·8	0·53	0·36	0·24	0·14	0·09

The optically thin and thick gas assumptions

An assessment was made of the transparent gas assumption (thin gas) and the diffusion approximation (thick gas) as a matter of interest. To do this the local radiative flux at the tube wall was computed for an assumed pressure of one atmosphere and a gas temperature distribution which was radially linear and invariant with axial position. The tube centerline temperature was taken as 500°R while the tube wall temperature was assumed to be 2500°R. The spectral absorption coefficients represented by equation (18) were used for the 4·3 μ band (only) of CO_2. According to the diffusion approximation the local radiative heat flux at the wall is given as

$$q_\nu/A = -\frac{2}{3}\left(\frac{\mathrm{d}E_{b\nu}}{\mathrm{d}\tau}\right)_{\text{local}} = -\frac{2}{3}\left[\frac{1}{\rho\kappa_\nu}\frac{\mathrm{d}E_{b\nu}}{\mathrm{d}T}\frac{\mathrm{d}T}{\mathrm{d}r}\right]_{\text{wall}} \quad (21)$$

while the transparent gas assumption produces the expression

$$q_\nu = \int_{\text{vol}} 4\rho\kappa_\nu[E_{b\nu} - (E_{b\nu})_w]\,\mathrm{d}V. \quad (22)$$

These expressions were used to produce the spectral results shown in Fig. 10. Superimposed on this figure are results (labeled "exact") which were produced by an uncoupled analysis with the use of a digital computer (see [10]).

CONCLUSIONS

1. The interaction of radiation with conduction and convection profoundly affects the temperature distribution for the conditions treated.

2. The axial component of radiation was found to have a negligible effect on the temperature distribution.

3. A "radiation boundary layer" was found to exist. This layer, which thickens in the flow direction, emits more radiation to the cool gas core than it absorbs from the hot wall. This net emission is more than compensated for by the conduction of heat from the wall.

4. For the hot wall–cold gas condition treated, the interaction or coupling of radiation with the conduction and convection mechanisms decreases both the local conduction and radiation at the wall. Thus the total heat flux at the wall, computed on a coupled basis, is significantly less than that computed on an uncoupled basis.

5. The uncoupled local convective heat flux (the Graetz problem) was found to be less than the coupled local total heat flux, at the wall, near the tube inlet. The two fluxes became equal at some downstream location (at approximately twenty-seven diameters). The uncoupled convective heat flux then becomes greater than the coupled total heat flux as the flow proceeds further downstream. At any given axial location, the bulk temperature given by the Graetz convection is lower than that indicated by the solution of the coupled problem.

6. A crude approach for predicting the total heat-transfer rate at the tube wall, based on the uncoupled convective heat-transfer coefficient (the Graetz problem) and a radiative flux based on the bulk mean temperature and total gas emissivities, produced results which were higher (by as much as a factor of two and one-half) than the total heat flux predicted with the use of the coupled program.

7. For the nongray gas and geometries treated, the optical density was very low at the band wings and very high at the band heads. Thus, although the transparent gas approximation correlated the spectral results obtained at the wing of the 4·3 μ band and the diffusion approximation correlated the results at the band head, neither of these approximations were found adequate for the entire band.

ACKNOWLEDGEMENTS

The author wishes to thank Professor D. K. Edwards of the Engineering Department at UCLA for defining the problem and providing fruitful discussions. Messrs. C. Vok, R. Van Wyk, and D. Rothman deserve grateful acknowledgement for their expert numerical techniques and computer program coding.

REFERENCES

1. R. GOULARD and M. GOULARD, Energy transfer in Couette flow of a radiant and chemically reacting gas, in *Proc. Heat Transf. Fluid Mech. Inst.* Stanford University Press, Stanford (1959).
2. R. VISKANTA and R. J. GROSH, Temperature distribution in Couette flow with radiation, *Am. Rocket Soc. J.* **31**, 839–840 (1961).
3. V. N. ADRIANOV and S. N. SHORIN, Radiant heat transfer in a flowing radiating medium, *Izv. Akad. Nauk SSSR, Otd. Tekh. Nauk* **5**, 46 (1958) (U.S. Atomic Energy Commission translation AEC-tr-3928).
4. T. H. EINSTEIN, Radiant heat transfer to absorbing gases enclosed in a circular pipe with conduction, gas flow, and internal heat generation, NASA TR R-156 (1963).
5. H. C. HOTTEL and E. S. COHEN, Radiant heat exchange in a gas filled enclosure, *A.I.Ch.E. Jl* **4**, 3–14 (1958).
6. L. D. NICHOLS, Temperature profile in the entrance region of an annular passage considering the effects of turbulent convection and radiation, *Int. J. Heat Mass Transfer* **8**, 589–607 (1965).
7. J. T. BEVANS and R. V. DUNKLE, Radiant interchange within an enclosure, *J. Heat Transfer* **82**, 1–9 (1960).
8. D. K. EDWARDS, Radiation interchange in a nongray enclosure containing carbon dioxide–nitrogen gas mixture, *J. Heat transfer* **84**, 1–11 (1962).
9. S. DESOTO, The radiation from an axisymmetric real gas system with a nonisothermal temperature distribution, *Chem. Engng Prog. Symp. Ser.* **61** (59), 138–154 (1965).
10. S. DESOTO and D. K. EDWARDS, Radiative emission and absorption in nonisothermal nongray gases in tubes, in *Proc. Heat Transf. Fluid Mech. Inst.* Stanford University Press, Stanford (1965).
11. J. R. HOWELL and M. PERLMUTTER, Monte Carlo solution of radiant heat transfer in a nongray nonisothermal gas with temperature dependent properties, AIChE National Meeting, preprint, San Juan, Puerto Rico (September 1963).
12. M. JAKOB, *Heat Transfer*. John Wiley, New York (1949).
13. J. R. SELLARS, M. TRIBUS and J. S. KLEIN, Heat transfer to laminar flow in a round tube or flat conduit—the Graetz problem extended, *Trans. Am. Soc. Mech. Engrs* **78**, 441–448 (1956).
14. G. M. BROWN, Heat or mass transfer in a fluid in laminar flow in a circular or flat conduit, *A.I.Ch.E. Jl* **6**, 179–183 (1960).
15. S. CHANDRASEKHAR, *Radiative Transfer*. Dover, New York (1960).
16. D. K. EDWARDS and W. A. MENARD, Correlations for absorption by methane and carbon dioxide gases, *Appl. Optics* **3**, 847–852 (1964).
17. H. C. HOTTEL, Radiant heat transmission, in *Heat Transmission*, by W. H. MCADAMS, 3rd edn., Chapter 4. McGraw-Hill, New York (1954).

Résumé—On expose une méthode théorique pour étudier l'interaction ou le couplage du rayonnement avec les mécanismes de conduction et de convection dans un écoulement de gaz non-gris et non-isotherme dans la région d'entrée d'un tube avec des parois noires et isothermes. On considère un écoulement établi hydrodynamiquement et laminaire. On a trouvé que le rayonnement modifie énergiquement la distribution de température et le transport de chaleur par convection dans l'écoulement cylindrique considéré. Ni l'hypothèse du gaz gris ni celle du gaz transparent ni l'approximation de la diffusion n'est demandée puisque l'on a trouvé que chacune était insufficante. Ainsi les effets d'absorption d'intercouche d'un gaz non gris et non isotherme sont pris en compte dans l'analyse. On a tenu compte à la fois du rayonnement des composantes axiale et radiale. On a utilisé un modèle exponentiel de bande pour représenter la dépendance en fonction de la température et de la fréquence des coefficients d'absorption spectrale.

L'analyse n'est pas restreinte à l'emploi du modèle exponentiel de bande employé, comme exemple satisfaisant, pour représenter les propriétés de rayonnement du CO_2. La formulation exacte de l'interaction du rayonnement, de la conduction et la convection dans un milieu non gris, émetteur et récepteur, et en écoulement est représentée par une équation intégrodifférentielle nonlinéaire qui a été résolue numériquement. Les résultats de diverses méthodes simplifiées de prévision ont été comparés avec les résultats exacts obtenus.

Zusammenfassung—Um die Wechselwirkung der Wärmestrahlung oder ihre Koppelung mit dem Mechanismus der Wärmeleitung und Konvektion in einem nicht-isothermen, nicht-grauen Gas, im Einlaufbereich eines Rohres mit schwarzen Wänden zu erforschen, wurde eine Berechnungsmethode entwickelt. Die Strömung wird laminar und hydrodynamisch ausgebildet angenommen. Es ergab sich, dass die Strahlung die Temperaturverteilung im Rohr und den konvektiven Wärmeübergang in dem betrachteten Bereich drastisch beeinflusst. Weder die Annahme eines grauen oder durchlässigen Gases noch die Diffusionsnäherung werden verwendet, da sich beide als ungeeignet erwiesen. So wird für die Berechnung die Absorption in einem nicht-grauen, nicht-isothermen Gas berücksichtigt. Sowohl die radiale als auch die axiale Komponente der Strahlung sind eingeschlossen. Um die Temperatur- und Frequenzabhängigkeit des Absorptionskoeffizienten zu berücksichtigen, wird ein Exponentialmodell für die Bande angenommen. Die Berechnung ist nicht auf dieses Modell beschränkt, welches, als günstigstes Beispiel, verwendet wurde, um die Strahlungseigenschaften von CO_2 wiederzugeben.

Die genaue Formulierung der Wechselwirkung von Strahlung, Leitung une Konvektion in einem fliessenden, nicht-grauen, emittierenden und absorbierenden Medium wird durch eine nichtlineare Integro-Differentialgleichung gegeben, die numerisch gelöst wurde. Die Ergebnisse verschiedener vereinfachter Berechnungsmethoden werden mit den genauen Ergebnissen dieser Gleichung verglichen.

Аннотация—Разработан аналитический метод исследования совместного излучения, теплопроводности и конвекции в потоке неизотермического несерого газа во входном участке трубы с изотермическими черными стенками. Поток считается гидродинамически развитым и ламинарным. Найдено, что излучение чрезвычайно сильно влияет на распределение температуры и конвективный теплообмен в поле исследуемого цилиндрического течения. В данном исследовании не привлекалось ни приближение серого газа, ни приближение прозрачного газа, ни диффузионное приближение, поскольку все они оказались направомерными. Таким образом, при анализе учитываются эффекты поглощения внутри среды из несерого неизотермического газа, а также осевая и радиальная лучистые составляющие. Для выражения зависимости коэффициентов спектрального поглощения от температуры и частоты использовалась экспоненциальная модель полосы. Анализ не ограничен применением этой модели, которая удачно иллюстрируется на примере применения для излучательных свойств CO_2. Точная формулировка взаимодействия излучения, теплопроводности и конвекции в движущейся несерой излучающей и поглощающей среде представлена интегро-дифференциальным уравнением, которое решено численно, Результаты различных упрощенных расчетных методов сравнивались с полученными точными результатами.